

- from *Xenopus laevis*: preparation of substrates and assay procedures. *Methods Enzymol.* **304**, 715–725 (1999).
20. Rundlett, S. E. *et al.* HDA1 and RPD3 are members of distinct yeast histone deacetylase complexes that regulate silencing and transcription. *Proc. Natl Acad. Sci. USA* **93**, 14503–14508 (1996).
21. Carmen, A. A., Rundlett, S. E. & Grunstein, M. HDA1 and HDA3 are components of a yeast histone deacetylase (HDA) complex. *J. Biol. Chem.* **271**, 15837–15844 (1996).
22. Guschin, D., Wade, P. A., Kikyo, N. & Wolffe, A. P. ATP-dependent histone octamer mobilization and histone deacetylation mediated by the Mi-2 chromatin remodeling complex. *Biochemistry* **39**, 5238–5245 (2000).
23. Pfeifer, G. P., Chen, H. H., Komura, J. & Riggs, A. D. Chromatin structure analysis by ligation-mediated and terminal transferase-mediated polymerase chain reaction. *Methods Enzymol.* **304**, 548 (1999).

Supplementary Information accompanies the paper on Nature's website (<http://www.nature.com/nature>).

Acknowledgements We thank D. Reinberg for the anti-RPB1 antibody; V. Sartorelli for the p300 expression construct; U. Schibler for Rev-Erbox reagents; H. R. Ueda for PATSER sequence analysis; and D. R. Weaver and C. L. Peterson for suggestions. This work was supported by grants from the NIH and the Defense Advanced Research Projects Agency (DARPA).

Competing interests statement The authors declare that they have no competing financial interests.

Correspondence and requests for materials should be addressed to S.M.R. (e-mail: steven.reppert@umassmed.edu).

IGF-1 receptor regulates lifespan and resistance to oxidative stress in mice

Martin Holzenberger*, Joëlle Dupont†, Bertrand Ducos*, Patricia Leneuve*, Alain Gëloën‡, Patrick C. Even§, Pascale Cervera|| & Yves Le Bouc*

* Institut National de la Santé et de la Recherche Médicale U515, and || Service d'Anatomie et de Cytologie Pathologiques, Hôpital Saint-Antoine, 75571 Paris 12, France

† Institut National de la Recherche Agronomique, 37380 Nouzilly, France

‡ Institut National de la Santé et de la Recherche Médicale U352, INSA, 69621 Villeurbanne, France

§ Institut National de la Recherche Agronomique, INA P-G, 75231 Paris 5, France

Studies in invertebrates have led to the identification of a number of genes that regulate lifespan, some of which encode components of the insulin or insulin-like signalling pathways^{1–3}. Examples include the related tyrosine kinase receptors InR (*Drosophila melanogaster*) and DAF-2 (*Caenorhabditis elegans*) that are homologues of the mammalian insulin-like growth factor type 1 receptor (IGF-1R). To investigate whether IGF-1R also controls longevity in mammals, we inactivated the IGF-1R gene in mice (*Igf1r*). Here, using heterozygous knockout mice because null mutants are not viable, we report that *Igf1r*^{+/-} mice live on average 26% longer than their wild-type littermates ($P < 0.02$). Female *Igf1r*^{+/-} mice live 33% longer than wild-type females ($P < 0.001$), whereas the equivalent male mice show an increase in lifespan of 16%, which is not statistically significant. Long-lived *Igf1r*^{+/-} mice do not develop dwarfism, their energy metabolism is normal, and their nutrient uptake, physical activity, fertility and reproduction are unaffected. The *Igf1r*^{+/-} mice display greater resistance to oxidative stress, a known determinant of ageing. These results indicate that the IGF-1 receptor may be a central regulator of mammalian lifespan.

Insulin/insulin-like signalling molecules that have been linked to longevity include DAF-2 and InR, and inactivation of the corresponding genes leads to increased lifespan in nematodes^{4,5} and

insects^{6,7}, respectively. Null mutations of the insect insulin-receptor substrate Chico, which acts downstream from InR, also extends lifespan⁸. Most long-lived *daf-2* and *Inr* mutants develop dwarfism and hypofertility; however, some *Inr* mutants display normal fertility and growth. This suggests that longevity may be regulated independently of body size and reproduction^{7,8}. DAF-2 and InR are structural homologues of a family of vertebrate tyrosine kinase receptors that includes the insulin receptor and the insulin-like growth factor type 1 receptor (IGF-1R). In vertebrates, the insulin receptor regulates energy metabolism⁹ whereas IGF-1R promotes growth¹⁰. IGF-1R is activated by its ligand IGF-I, which is secreted in response to growth hormone. It is unclear whether the insulin receptor or IGF-1R, or both, have taken over responsibility for lifespan regulation in vertebrates^{3,8}. The phenotypes of long-lived spontaneous mouse mutants studied so far indicate a probable link between longevity and growth. The long-lived *Prop1*^{dw/dw} (Ames dwarf) and *Pit1*^{dw/dw} (Snell dwarf) mutants^{11,12} display impaired pituitary gland development and low levels of pituitary hormones, including growth hormone. These mutants are sterile dwarfs. The recent targeted inactivation of the growth hormone receptor itself,

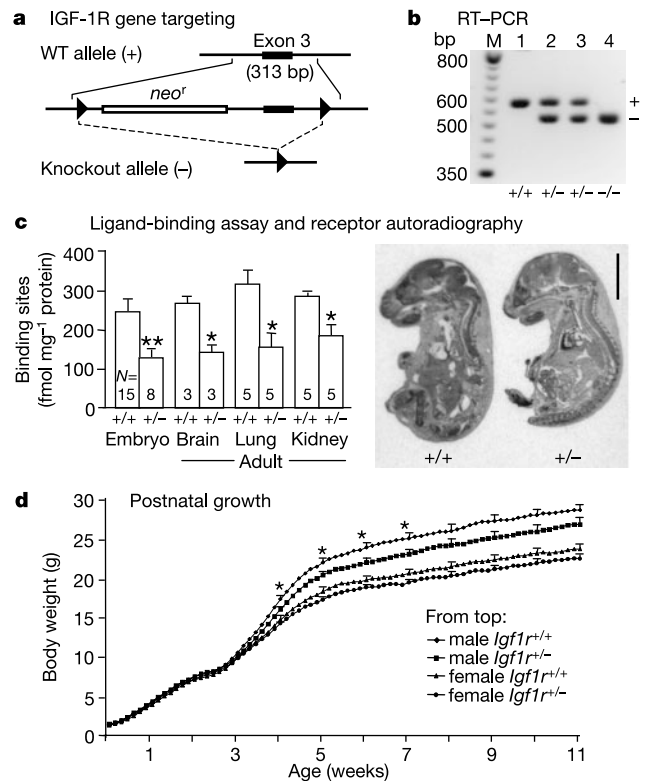


Figure 1 IGF-1R gene targeting, receptor expression and growth phenotype. **a**, We flanked exon 3 of the wild-type (WT) IGF-1R gene with a neomycin-resistance cassette (*neo^r*) and two loxP sites (triangles). Exon 3 and *neo^r* were then deleted by *Cre-lox* recombination, producing the *Igf1r*⁻ (knockout) allele^{14,15}. **b**, Allele-specific RT-PCR²⁵ revealed that heterozygous *Igf1r*^{+/-} mice produced mRNA from wild-type (+) and knockout (-) alleles (double band in lanes 2 and 3). M, DNA size marker. **c**, Although levels of IGF-1R were halved in *Igf1r*^{+/-} animals (bar graph), the relative distributions (autoradiographic pattern) were unchanged. Receptors were undetectable in *Igf1r*^{-/-} embryos (data not shown). Together, this indicates that the remaining, intact allele does not compensate for its inactivated homologue. Nonspecific binding was 8%. Scale bar, 5 mm. Asterisk, $P < 0.05$; double asterisk, $P < 0.01$ (Mann-Whitney *U*-test). See also Supplementary Information. **d**, *Igf1r*^{+/-} and wild-type siblings show identical growth until day 20. Thereafter, during the prepubescent growth spurt (weeks 3–5), slight deficits appear. Asterisk, $P < 0.05$ (Mann-Whitney *U*-test).

which strongly decreases circulating IGF-I and impairs growth and development, also increases lifespan¹³. Similarly, caloric restriction, the only efficient treatment known to increase mammalian lifespan, invariably reduces circulating IGF-I levels, and, if begun in juveniles, also engenders dwarfism. These findings led us to investigate whether mammalian lifespan is regulated by IGF-1R.

We inactivated the IGF-1R gene by homologous recombination using the *Cre-lox* strategy to delete the essential exon 3 of the gene^{14,15} (Fig. 1a). We found that homozygous null mutants (*Igf1r*^{-/-}) died at birth, as previously described in a study using classical insertional mutagenesis¹⁶. Our *Igf1r*^{+/-} mutant transmitted the null allele in the expected mendelian ratio (52%, *n* = 241). Wild-type and *Igf1r*-null transcripts were present (Fig. 1b); however, as *Igf1r*-null transcripts cannot be translated into functional protein¹⁵, IGF-1 receptor levels in *Igf1r*^{+/-} mice were half those in wild type *Igf1r*^{+/+} mice (Fig. 1c). Weight at birth and during the first three weeks of growth were nevertheless normal (Fig. 1d). Only after the natural weaning period (around day 20) did *Igf1r*^{+/-} males develop a modest, 8% growth deficit with respect to their *Igf1r*^{+/+} littermates (23.1 ± 0.7 g compared with 25.1 ± 0.7 g at age 7 weeks, *P* < 0.05), whereas the growth deficit did not exceed 6% in females (19.5 ± 0.6 g compared with 20.7 ± 0.5 g at 7 weeks, not significant (NS)). These modest weight differences affected all tissues to similar degrees, persisted throughout life (data not shown), and resembled the growth pattern observed in previous models of partial inactivation of the IGF-1R gene¹⁵. Thus, the bi-allelically expressed mouse IGF-1R gene is heteroinsufficient.

Fed *ad libitum* on a standard diet and maintained in regular housing until natural death, mice with only one functional IGF-1R allele significantly outlived their wild-type littermates (Fig. 2). *Igf1r*^{+/-} mice lived a mean of 26% longer than *Igf1r*^{+/+} controls (*P* < 0.02; Cox's test). If the sexes were evaluated separately, mutant females were found to live 33% longer than wild-type females (*P* < 0.001), whereas mutant males lived only 15.9% longer than

control males (NS). On average, *Igf1r*^{+/-} females outlived *Igf1r*^{+/-} males, whereas the opposite is normally the case in wild-type populations of the 129/J genetic background¹⁷ (Fig. 2). Thus, in *Igf1r*^{+/-} mice, the degree to which lifespan is extended depends on sex, as has been described for *Drosophila* mutants with impaired insulin-like signalling^{6,8}. Our ageing cohorts had a 5% tumour incidence, unrelated to genotype and consistent with the low (7%) general tumour incidence of mice with the 129/J background^{18,19}. Necropsy revealed a number of different diseases, consistent with the results of previous studies, showing that mice with this background do not develop specific age-related diseases¹⁹. We did not observe accidental deaths, although some of the sporadic mortality of younger males may have been consequences of fights for dominance.

Blood parameters (see Methods) were normal. However, serum IGF-I levels were upregulated in adult *Igf1r*^{+/-} mice (males, 795 ± 64 compared with 625 ± 30 ng ml⁻¹, *P* < 0.01; females, 716 ± 39 compared with 516 ± 14 ng ml⁻¹, *P* < 0.001; *n* = 8–10 per group) and may reflect an endocrine response to the reduced availability of IGF-1R¹⁵. Blood glucose levels in mice that were deprived of food overnight were unaffected. In fed animals, however, *Igf1r*^{+/-} males tended to have higher (+12%) and *Igf1r*^{+/-} females to have lower (-4.4%) blood glucose levels than the controls. Non-fasting insulin levels were nevertheless normal (males, 1.65 ± 0.12 compared with 1.40 ± 0.14 ng ml⁻¹; females, 1.58 ± 0.25 compared with 1.90 ± 0.25 ng ml⁻¹; *n* = 8–10 per group). We then tested glucose tolerance in mice that were deprived of food overnight (Fig. 3a, b) and found that *Igf1r*^{+/-} males had a significantly stronger glucose response than controls (*P* < 0.001). In *Igf1r*^{+/-} females, the response was slightly weaker than in wild-

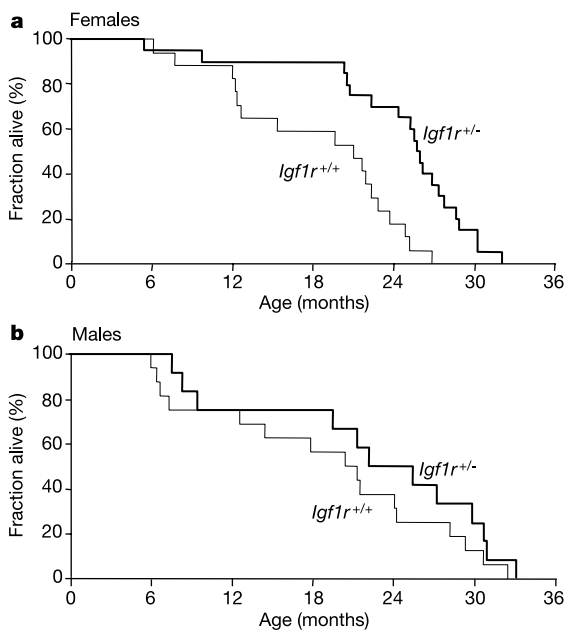


Figure 2 Lifespan extension in *Igf1r*^{+/-} mice with respect to *Igf1r*^{+/+} (WT) mice. **a**, *Igf1r*^{+/-} females (thick line) live a mean of 33% longer than their wild-type littermates (756 ± 46 compared with 568 ± 49 days; *P* < 0.01, *t*-test). Kaplan–Meier analysis of survival revealed a later decline in *Igf1r*^{+/-} mice compared with wild type (*P* < 0.001, Cox's test). **b**, *Igf1r*^{+/-} males live 15.9% longer than wild-type littermates (679 ± 80 compared with 585 ± 69 days; NS).

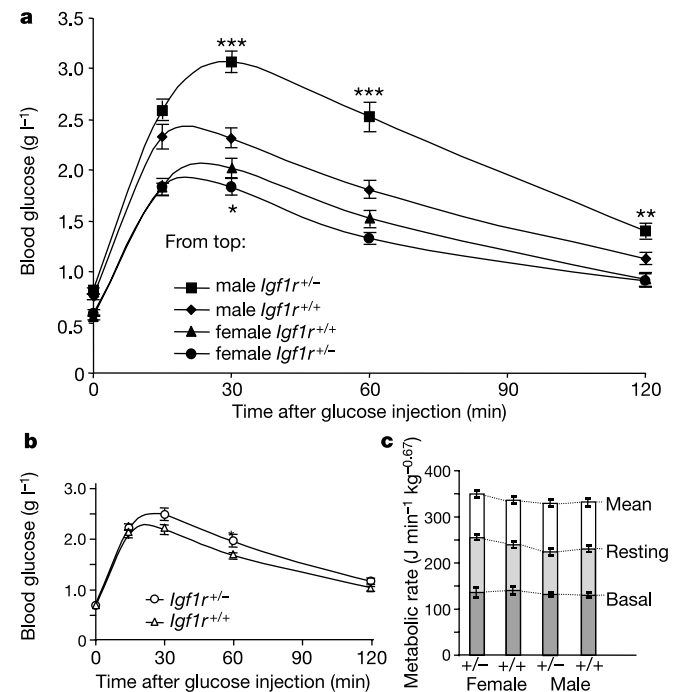


Figure 3 Glucose tolerance and energy metabolism in *Igf1r*^{+/-} mice. **a**, After an intraperitoneal glucose injection, the glucose response is strongest in mutant males. Note that the significant sex-related dimorphism of the response observed in wild-type mice is even more marked between mutants. Asterisk, *P* < 0.05; double asterisk, *P* < 0.01; triple asterisk, *P* < 0.001. **b**, Combining data from both sexes largely cancels out the male hyperglycaemic phenotype. Asterisk, *P* < 0.05; *n* = 89. **c**, Metabolic rate, measured by indirect calorimetry, did not differ between groups whether we determined mean (24 h), resting or basal metabolic rate (*n* = 11–12 per group).

type females ($P < 0.05$). It remains unclear whether this hyperglycaemic effect in *Igf1r*^{+/-} males is related to the reportedly compromised β -cell mass in these mice²⁰.

As metabolism may have an important role in ageing, we explored energy expenditure in *Igf1r*^{+/-} mice. Body temperature, indicative of metabolic activity and reported to be low in long-lived Ames dwarf mice²¹, was unaffected in *Igf1r*^{+/-} mice: skin surface temperature was $36.1 \pm 0.1^\circ\text{C}$ for all 4 groups ($n = 9\text{--}14$ per group) and rectum temperature was 37.4 ± 0.2 compared with $37.5 \pm 0.2^\circ\text{C}$ in males and 37.7 ± 0.2 compared with $37.9 \pm 0.2^\circ\text{C}$ in females (NS). We analysed physical activity, using a photoelectric actimeter, and found identical circadian profiles for *Igf1r*^{+/-} and *Igf1r*^{+/+} mice (data not shown). Further-

more, as caloric restriction is known to extend rodent lifespan, we investigated the possibility that *Igf1r*^{+/-} mice were able to restrict their own food intake. We measured short-term (1–3 days) and long-term (90 days) food intake in adults. We observed only marginal differences between *Igf1r*^{+/-} and *Igf1r*^{+/+} mice, with mean food intake (in $\text{g d}^{-1}\text{kg}^{-1}$ body weight) being 190 ± 2 compared with 204 ± 4 (NS) in males and 148 ± 4 compared with 144 ± 2 (NS) in females, and mean water intake (in $\text{ml d}^{-1}\text{kg}^{-1}$ body weight) being 249 ± 7 compared with 255 ± 29 (NS) in males and 178 ± 4 compared with 166 ± 3 (NS) in females.

As mice may use nutrients with variable efficiency, we determined their metabolic rates. We obtained similar mean metabolic rates in fed animals over 24 h (males, 332.8 ± 6.7 compared with $336.0 \pm 8.4 \text{ J min}^{-1} \text{ kg}^{-0.67}$; females, 351.9 ± 6.0 compared with $337.9 \pm 7.0 \text{ J min}^{-1} \text{ kg}^{-0.67}$; NS, $n = 11\text{--}12$ per group) (Fig. 3c). The resting metabolic rate was also similar between mutants and controls. As the difference between resting and 24-h metabolic rate depends mainly on physical activity, these results are consistent with the observed identical activity profiles. Even basal metabolic rate, measured in the fasted state, did not differ between mutants and controls (males, 133.2 ± 5.3 compared with $132.0 \pm 4.7 \text{ J min}^{-1} \text{ kg}^{-0.67}$; females, 135.8 ± 9.4 compared with $140.9 \pm 6.6 \text{ J min}^{-1} \text{ kg}^{-0.67}$).

Long-lived *C. elegans daf-2* mutants and long-lived dwarf mice display changes in fertility. We therefore monitored fertility and reproduction in *Igf1r*^{+/-} female mice from puberty to the age of 13 months. *Igf1r*^{+/-} females became fertile at 5.2 ± 0.1 weeks whereas *Igf1r*^{+/+} females became fertile at 5.6 ± 0.3 weeks (5.8 ± 0.1 compared with 6.2 ± 0.3 in males; $n = 7\text{--}11$ per group). Although these differences were not significant, *Igf1r*^{+/-} mice became fertile,

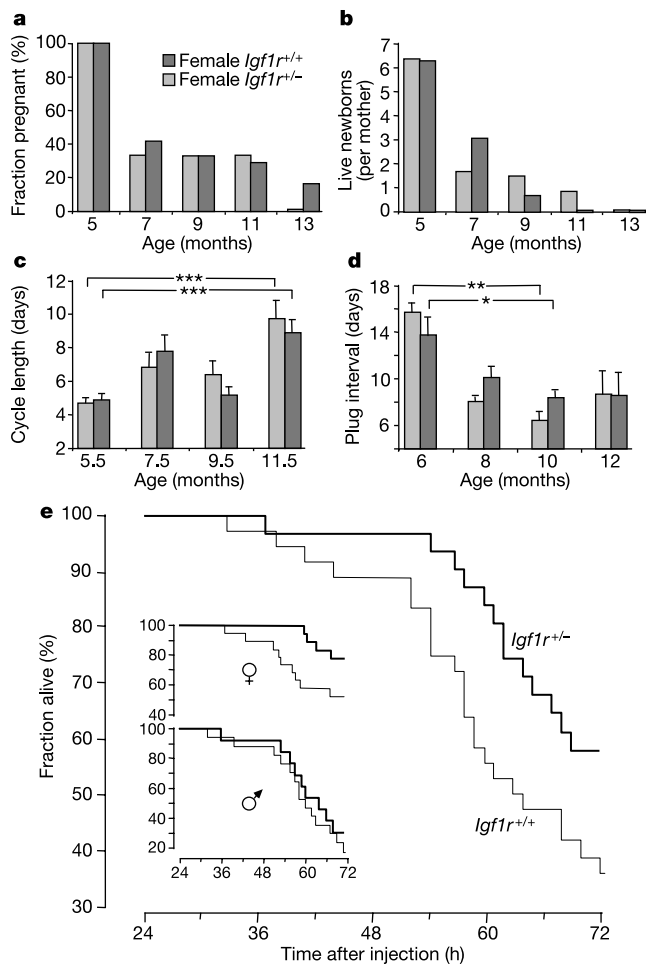


Figure 4 Mutants show normal fertility and are resistant to oxidative stress. **a**, Three-week mating results in a similar proportion of pregnancies in mutant and wild-type females. These proportions decline from 5 to 13 months of age ($P < 0.001$, χ^2 test). **b**, Although offspring decrease markedly with age, there are no consistent differences between *Igf1r*^{+/-} and control females. **c**, Oestrus cycle length increases significantly with age (triple asterisk, $P < 0.005$), reflecting changes in the hormonal control of ovarian function, but we observed no differences between genotypes. **d**, The interval between the first copulation plug (from a sterile male) and the next, indicative of ovarian capacity to maintain pseudogestation, decreases significantly with age in both groups. Asterisk, $P < 0.05$; double asterisk, $P < 0.02$; $n = 15$. **e**, Oxidative stress is induced by intraperitoneal paraquat injection (70 mg per kg body mass). We checked the mice every 2 h and censored the test at 72 h. Kaplan–Meier analysis shows significantly more survivors among *Igf1r*^{+/-} mice ($P < 0.05$, Cox's test; $n = 67$). When evaluated separately (inset), female mutants exhibit increased stress resistance ($P = 0.05$, log-rank test; $n = 37$), whereas the increase in males ($n = 30$) is small.

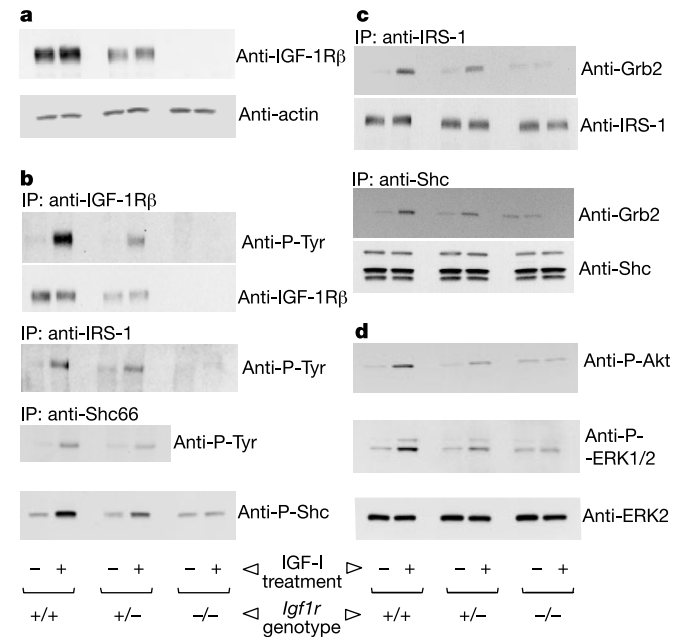


Figure 5 Lack of IGF-1R reduces activation of major intracellular signalling pathways in cultured MEFs. We stimulated MEFs with rhIGF-I (+) and analysed them by western blot. **a**, IGF-1R was reduced in *Igf1r*^{+/-} and absent from *Igf1r*^{-/-} MEFs. **b**, Anti-IGF-1R β , anti-IRS-1 and anti-p66 Shc immunoprecipitates (IP) were probed with anti-phosphotyrosine (anti-P-Tyr) antibodies. Phosphorylation of these proteins was reduced in *Igf1r*^{+/-} and absent from *Igf1r*^{-/-} MEFs. A phospho-Shc antibody revealed reduced activation of p52 Shc. **c**, **d**, IGF-I-induced association of Grb2 with IRS-1 or p52 Shc, and activation of ERK1/2 MAP kinases and Akt, are also reduced in *Igf1r*^{+/-} and absent from *Igf1r*^{-/-} MEFs.

on average, 3 days earlier than controls. This suggests that IGF-1R insufficiency does not delay sexual maturation, in contrast to the growth hormone receptor and binding protein (GHR/BP) knockout¹³. The litter size of young *Igf1r*^{+/-} females was 6.3 ± 0.5 ($n = 7$ litters), which is not different from wild-type 129/Sv females (6.4 ± 0.2 live newborns; $n = 120$ litters). We analysed the age-related decline in female fertility, determining frequency of pregnancies, number of live newborns, mating behaviour, oestrus cycle length and ovarian capacity to maintain pseudogestation (Fig. 4a–d). As expected, fertility decreased markedly with age, but *Igf1r*^{+/-} females and their controls displayed indistinguishable profiles.

Oxidative stress is a principal cause of ageing²², and mouse and fly mutants with enhanced resistance to oxidative stress are long-lived^{23,24}. We therefore subjected adult mice to oxidative stress by injection of paraquat, a herbicide that induces formation of reactive oxygen species. *Igf1r*^{+/-} mutants resisted this challenge significantly longer than controls (Fig. 4e). This increase in stress resistance seemed to be more pronounced in female than in male mutants (Fig. 4e, inset). To further substantiate these results, we induced oxidative damage in cultured mouse embryonic fibroblasts (MEFs) by low concentrations of H₂O₂, and found that the proportion of surviving cells was significantly higher in *Igf1r*^{+/-} than in control MEFs after 24- and 72-h treatments (24 h, $94\% \pm 3$ compared with $82\% \pm 3$, $P < 0.02$; 72 h, $88\% \pm 3$ compared with $68\% \pm 2$, $P < 0.001$).

Mutations of the *Drosophila* IRS homologue Chico⁸ and of other proteins acting downstream of IGF-1R, such as mouse p66 Shc²³ and *C. elegans* phosphatidylinositol-3-OH kinase (AGE-1)¹, but also regulation of forkhead transcription factor DAF-16 by Akt, increase lifespan. We therefore investigated how the reduced IGF-1R levels affected intracellular signalling in this model. We derived embryonic fibroblasts from wild type, *Igf1r*^{+/-} and *Igf1r*^{-/-} mice^{14,15} and studied signalling by western blot. As expected, *Igf1r*^{+/-} cells showed 50% reduction in IGF-1R levels (Fig. 5a). Immunoprecipitation and western analysis also showed a marked reduction in IGF-I-induced tyrosine phosphorylation of IGF-1R and of its substrate IRS-1 (Fig. 5b). The tyrosine phosphorylation of both p52 and p66 isoforms of Shc, another major substrate of IGF-1R, were also reduced by half (Fig. 5b). This is of interest as reduced p66 Shc activation in *Igf1r*^{+/-} cells could be a mechanism by which IGF-I regulates oxidative stress resistance. Shc and IRS-1 bind Grb2 on phosphorylation and thereby activate the mitogen-activated protein (MAP) kinase pathway, involved in mitogenic response. The amount of Grb2 co-immunoprecipitating with p52 Shc or IRS-1 are reduced to half in *Igf1r*^{+/-} cells (Fig. 5c). Two important pathways activated by IGF-I are the MAP kinase ERK1/2 and phosphatidylinositol-3-OH kinase/Akt kinase signalling cascades. Consistently, IGF-I-stimulated phosphorylation of ERK1/2 and Akt is reduced by 40–50% in mutant cells (Fig. 5d). Together, this suggests that IGF-1R heteroinsufficiency downregulates the principal pathways stimulated by IGF-I.

These results show that a general decrease in IGF-1 receptor levels can increase lifespan in a mammalian species. Thus, the genetic link between insulin-like signalling and longevity, originally discovered in non-vertebrates^{4–6}, also seems to exist in higher vertebrates. Unlike long-lived mouse mutants with hypopituitarism^{11,12,25} or with complete lack of GHR/BP¹³, long-lived *Igf1r*^{+/-} mutants, in which receptor levels were only reduced by 50%, did not develop dwarfism or hypofertility. We obtained these results using a 129/Sv genetic background. Preliminary results, however, using an IGF-1R knockdown mutation¹⁵ on a hybrid background (129/Sv × C57Bl/6J) confirm our findings on lifespan extension (M.H., unpublished data). IGF-1R is involved in the regulation of carbohydrate metabolism and in the pancreatic control of glucose homeostasis²⁶. It is therefore not surprising that we found abnormal regulation of blood glucose in *Igf1r*^{+/-} mice. This abnormality affects only

males and is clearly a sex-related dimorphism. Reduced glucose tolerance is a symptom of prediabetes, and its potential consequences may have masked an otherwise possibly greater life-prolonging effect of IGF-1R insufficiency in males. We have observed previously other gender-related phenotypic differences in IGF-1R mutants^{14,15}, and have proposed the interplay of sex-dimorphic pulsatile growth hormone regulation, paracrine secretion and signalling of IGF-I, and androgen/oestrogen actions at the target cell level as possible explanations. Furthermore, similar sex dimorphism of longevity has been reported in *InR* mutant *Drosophila* and in long-lived Ames dwarf mice^{6,12}. It is tempting to speculate on the physiological significance of this sex dimorphism because major sex differences in lifespan have been found in numerous species, but clearly additional studies are needed. We thought that the observed variations in blood glucose might have had consequences for energy metabolism and expenditure, and that these mice might present features of caloric restriction. However, we show that *Igf1r*^{+/-} mice have normal food uptake, physical activity or metabolic rate, which excludes metabolic differences as the cause of their longevity. It is, on the contrary, possible that the life-prolonging effects of caloric restriction are due to decreases in circulating IGF-I levels, mimicking the IGF-1R insufficiency produced here.

p66 Shc^{-/-} is the only other targeted mutation in mammals described so far that leads to a comparable increase in lifespan without inducing major side effects²³. The p66 isoform of Shc mediates cellular responses to oxidative stress and is, together with IRS-1, a major cytoplasmic signal transduction molecule for IGF-1R. Thus, the resistance of *Igf1r*^{+/-} mice to oxidative stress is of considerable interest, and by showing that the stress-regulating p66 Shc is underphosphorylated in IGF-1R deficiency we found a plausible mechanism connecting IGF signalling to oxidative stress. Caloric restriction and decreases in the response to oxidative stress and in insulin-like growth factor signalling all efficiently extend lifespan in mice. However, it is unclear how these mechanisms cooperate and the extent to which they are independent. Data from *Drosophila chico*¹ mutants showing that lifespan is extended much more than can be explained by the modest increase in resistance to oxidative stress⁸ suggested that the two mechanisms operate independently, at least in part, to generate longevity. However, the issue of cooperation and independence of caloric restriction, insulin-like signalling and oxidative stress in lifespan extension remains unclear^{25,27}. Owing to strong oxidative stress-resistance phenotypes associated with *C. elegans* longevity mutations²⁸, these aspects merit further study in vertebrates. Our *Igf1r*^{+/-} mutants provide an invaluable tool for future exploration of the mechanisms of lifespan regulation. However, it will also be necessary to try to overproduce IGF antagonists, to administer inhibitors of IGF-1R activation, or to block signal transduction. It has recently been shown that lifespan regulation through insulin-like signals in non-vertebrates probably occurs in a non-cell-autonomous fashion²⁹. Neurons in the central nervous system, by sensing the circulating levels of ligand, may have a central function in regulating the ageing of other tissues by means of hypothetical endocrine mechanisms. We have begun to investigate this possibility in a mammalian model, using the *Cre-lox* approach to produce brain-specific IGF-1R knockout mice. Homozygous mice for this mutation are microcephalic, sterile, and have a complex neuroendocrine dysfunction, but heterozygous mice are healthy and are useful for lifespan studies. □

Methods

Mice

The *Igf1r* mutant, described elsewhere¹⁴ and available from <http://www.emma.rm.cnr.it>, was maintained in the heterozygous state in the 129/Sv genetic background. By mating *Igf1r*^{+/-} males with 9- to 12-week-old 129/Sv wild-type females, we generated three cohorts, each composed of heterozygous *Igf1r*^{+/-} and *Igf1r*^{+/+} (wild type) littermates. Animals lived in conventional conditions: 23 °C, 14/10-h light/dark cycle, standard diet

(49% carbohydrates, 24% proteins, 5% lipids, 12% humidity, 10% minerals and fibre) and water *ad libitum*. We separated mice from mothers on day 30 and grouped them as 6 males or 6 females per cage, with both genotypes present in each cage. Mice from cohort 1 (20 *Igflr*^{+/-} and 17 *Igflr*^{+/+} females; 12 *Igflr*^{+/-} and 16 *Igflr*^{+/+} males) were checked daily but otherwise left undisturbed until they died naturally. Single surviving females were placed in the neighbouring cage, whereas single surviving males received a female for company. We performed necropsy whenever possible, including tumour immunohistochemistry. Four animals were killed when death appeared imminent, to reduce suffering. We drew Kaplan–Meier survival curves using dates of birth and death. Cohort 2 (9 *Igflr*^{+/-} and 15 *Igflr*^{+/+} females; 14 *Igflr*^{+/-} and 11 *Igflr*^{+/+} males) was used for blood biochemistry and analysis of glucose tolerance, food consumption, fertility and body composition. In cohort 3 (17 *Igflr*^{+/-} and 11 *Igflr*^{+/+} females, 14 *Igflr*^{+/-} and 15 *Igflr*^{+/+} males) we analysed growth, energy expenditure (by indirect calorimetry), blood parameters, glucose tolerance, and finally *in vivo* resistance to oxidative stress induced by methyl viologen (paraquat) injection. We conducted experiments according to institutional guidelines for care of laboratory animals.

IGF-1 receptor expression

Recombinant human IGF-I (rhIGF-I, for *in vitro* ligand-binding assays, described elsewhere^{14,15}) and rhdes(1-3)IGF-I (for autoradiography) were labelled with ¹²⁵I (see also Supplementary Information).

For the allele-specific expression assay, we used total RNA from *Igflr*^{+/-} embryos and triplex reverse transcriptase-polymerase chain reaction (RT-PCR)²⁶. We co-amplified corresponding fragments from the coding region of the messenger RNA specific for the wild-type and the inactivated receptor allele. The single forward primer 5'-CGCCTGAAAAGTGCACG-3' annealed with exon 2, the first reverse primer 5'-AGCTGCCAGGCACTCCG-3' annealed with exon 3, and the second reverse primer 5'-GCAGGGATACAGTACATGTTT-3' spanned the knockout-specific splice junction between exons 2 and 4. RT-PCR products of 518 base pairs (bp) corresponded to the transcript of the knockout allele, and 574-bp products corresponded to wild type. We extracted total RNA from embryo homogenates by RNAXEL and performed One-Step RT-PCR using GeneAmp 2400 cyclers. For the reverse transcription reaction, we incubated 30 ng total RNA at 50 °C for 30 min and at 94 °C for 2 min, followed by 40 PCR cycles, each consisting of 30-s segments at 94, 59 and 72 °C.

Postnatal growth

To synchronize individual growth, we recomposed 7 litters (cohort 3) on day 1 to yield 8 or 9 pups per mother. We identified newborn mice with coloured ink and permanently numbered them on day 8. For 11 weeks we weighed them daily at 16:00 on an electronic balance. Growth curves used sliding means of present weight and weight on the day before and after.

Fertility

We determined the onset of male and female fertility by mating *Igflr*^{+/-} and *Igflr*^{+/+} mice from day 30 onwards with fertile wild-type partners (three females per male). The age of delivery and litter size (when testing females) were compared between genotypes. To evaluate the decline in female fertility over time we used three sets of parameters. Measurements started at 5 months of age and were repeated 3 or 4 times at 2-month intervals. First, we monitored the oestrus cycle by vaginal smear histology for 18 days. Second, we analysed sexual behaviour and the duration of pseudogestation by mating females for 2 weeks with vasectomized males and recording vaginal plugs. Third, we mated females with fertile males for three weeks and recorded the resulting pregnancies and offspring.

Blood tests

We measured total bilirubin, cholesterol, creatinine, glucose, lactate, total protein, triglycerides, urea and uric acid in 5-month-old mice. Circulating IGF-I was measured using a double-antibody RIA from Diagnostic Systems Laboratories and plasma insulin using the Linco Sensitive Rat Insulin RIA. We tested glucose tolerance in mice that had gone without food for 14 h overnight by intraperitoneal injection with 2 g kg⁻¹ body weight of 25% D-glucose. We measured circulating glucose in tail blood at 0, 15, 30, 60 and 120 min using Lifescan Glucotouch.

Indirect calorimetry

We determined metabolic rate by indirect 24-h calorimetry (see Supplementary Information for details).

Experiments using MEFs

We established female MEFs from *Igflr*^{+/+}, *Igflr*^{+/-} and *Igflr*^{-/-} embryonic day (E)14 fetuses. IGF signalling pathways and *in vitro* resistance to H₂O₂ were studied in early passages of MEFs. For IGF signalling we removed serum (10% FCS) from MEF cultures 16 h before analysis. Cells were stimulated with 3 nM rhIGF-I (Genentech) for 10 min before analysis, except for detection of phosphorylated Shc (5 min). For H₂O₂ resistance we treated MEFs with 100 μM H₂O₂ and determined cell viability after 1–3 days using Trypan blue and a haemocytometer. *n* = 6 for each group, in two independent experiments.

Western blotting

We performed immunoprecipitation and western blotting as described³⁰ (see Supplementary Information for details).

Statistics

For group comparisons, we used Student's *t*-test. Means are expressed ± standard error of the mean (s.e.m.). Error bars represent the s.e.m. We determined the significance of survival curves by Cox's test. We used nonparametric Mann–Whitney and χ² tests where indicated.

Received 4 October; accepted 18 November 2002; doi:10.1038/nature01298.

Published online 4 December 2002.

- Guarente, L. & Kenyon, C. Genetic pathways that regulate ageing in model organisms. *Nature* **408**, 255–262 (2000).
- Kenyon, C. A conserved regulatory system for aging. *Cell* **105**, 165–168 (2001).
- Gems, D. & Partridge, L. Insulin/IGF signalling and ageing: seeing the bigger picture. *Curr. Opin. Genet. Dev.* **11**, 287–292 (2001).
- Kimura, K. D., Tissenbaum, H. A., Liu, Y. & Ruvkun, G. Daf-2, an insulin receptor-like gene that regulates longevity and diapause in *Caenorhabditis elegans*. *Science* **277**, 942–946 (1997).
- Tissenbaum, H. A. & Ruvkun, G. An insulin-like signaling pathway affects both longevity and reproduction in *Caenorhabditis elegans*. *Genetics* **148**, 703–717 (1998).
- Tatar, M. *et al.* A mutant *Drosophila* insulin receptor homolog that extends life-span and impairs neuroendocrine function. *Science* **292**, 107–110 (2001).
- Bartke, A. Mutations prolong life in flies; implications for aging in mammals. *Trends Endocrinol. Metab.* **12**, 233–234 (2001).
- Clancy, D. J. *et al.* Extension of life-span by loss of CHICO, a *Drosophila* insulin receptor substrate protein. *Science* **292**, 104–106 (2001).
- Kulkarni, R. N. *et al.* Tissue-specific knockout of the insulin receptor in pancreatic beta cells creates an insulin secretory defect similar to that in type 2 diabetes. *Cell* **96**, 329–339 (1999).
- Lupu, L., Terwilliger, J. D., Lee, K., Segre, G. V. & Efstratiadis, A. Roles of growth hormone and insulin-like growth factor 1 in mouse postnatal growth. *Dev. Biol.* **229**, 141–162 (2001).
- Flurkey, K., Papaconstantinou, J., Miller, R. A. & Harrison, D. E. Lifespan extension and delayed immune and collagen aging in mutant mice with defects in growth hormone production. *Proc. Natl Acad. Sci. USA* **98**, 6736–6741 (2001).
- Brown-Borg, H. M., Borg, K. E., Meliska, C. J. & Bartke, A. Dwarf mice and the ageing process. *Nature* **384**, 33 (1996).
- Coschigano, K. T., Clemmons, D., Bellushi, L. L. & Kopchick, J. J. Assessment of growth parameters and life span of GHR/BP gene-disrupted mice. *Endocrinology* **141**, 2608–2613 (2000).
- Holzenberger, M. *et al.* Experimental IGF-1 receptor deficiency generates a sexually dimorphic pattern of organ-specific growth deficits in mice, affecting fat tissue in particular. *Endocrinology* **142**, 4469–4478 (2001).
- Holzenberger, M. *et al.* A targeted partial invalidation of the insulin-like growth factor I receptor gene in mice causes a postnatal growth deficit. *Endocrinology* **141**, 2557–2566 (2000).
- Liu, J. P., Baker, J., Perkins, A. S., Robertson, E. J. & Efstratiadis, A. Mice carrying null mutations of the genes encoding insulin-like growth factor I (*Igf-1*) and type 1 IGF receptor (*Igflr*). *Cell* **75**, 59–72 (1993).
- Storer, J. B. Longevity and gross pathology at death in 22 inbred mouse strains. *J. Gerontol.* **21**, 404–409 (1966).
- Stevens, L. C. & Little, C. C. Spontaneous testicular teratomas in an inbred strain of mice. *Proc. Natl Acad. Sci. USA* **40**, 1080–1087 (1954).
- Smith, G. S., Walford, R. L. & Mickey, M. R. Lifespan and incidence of cancer and other diseases in selected long-lived inbred mice and their F1 hybrids. *J. Natl Cancer Inst.* **50**, 1195–1213 (1973).
- Whithers, D. J. *et al.* Irs-2 coordinates IGF-1 receptor-mediated β-cell development and peripheral insulin signalling. *Nature Genet.* **23**, 32–39 (1999).
- Hunter, W. S., Croson, W. B., Bartke, A., Gentry, M. V. & Meliska, C. J. Low body temperature in long-lived Ames dwarf mice at rest and during stress. *Physiol. Behav.* **67**, 433–437 (1999).
- Finkel, T. & Holbrook, N. J. Oxidants, oxidative stress and the biology of ageing. *Nature* **408**, 239–247 (2000).
- Migliaccio, E. *et al.* The p66^{shc} adaptor protein controls oxidative stress response and life span in mammals. *Nature* **402**, 309–313 (1999).
- Sun, J. & Tower, J. FLP recombinase-mediated induction of Cu/Zn-superoxide dismutase transgene expression can extend the life span of adult *Drosophila melanogaster* flies. *Mol. Cell Biol.* **19**, 216–228 (1999).
- Bartke, A. *et al.* Extending the lifespan of long-lived mice. *Nature* **414**, 412 (2001).
- Kulkarni, R. N. *et al.* β-cell specific deletion of the IGF-1 receptor leads to hyperinsulinemia and glucose intolerance but does not alter β-cell mass. *Nature Genet.* **31**, 111–115 (2002).
- Clancy, D. J., Gems, D., Hafen, E., Leivers, S. J. & Partridge, L. Dietary restriction in long-lived dwarf flies. *Science* **296**, 319 (2002).
- Honda, Y. & Honda, S. Oxidative stress and life span determination in the nematode *Caenorhabditis elegans*. *Ann. NY Acad. Sci.* **959**, 466–474 (2002).
- Wolkow, C. A., Kimura, K. D., Lee, M. S. & Ruvkun, G. Regulation of *C. elegans* life-span by insulinlike signaling in the nervous system. *Science* **290**, 147–150 (2000).
- Dupont, J., Karas, M. & LeRoith, D. The potentiation of estrogen on insulin-like growth factor I action in MCF-7 human breast cancer cells includes cell cycle components. *J. Biol. Chem.* **275**, 35893–35901 (2000).

Supplementary Information accompanies the paper on Nature's website (<http://www.nature.com/nature>).

Acknowledgements We thank P. Monget for contributions to the experimental design; N. R. Holzenberger for assistance with metabolic and growth studies; G. Hamard for help with MEFs; J. Sappa for language revision; F. Veinberg for blood biochemistry; and P. Casanovas and M.-C. Samson for animal care. MENRT sponsored this study with a grant to M.H. and Y.L.B. We thank D. LeRoith for support to J.D.

Competing interests statement The authors declare that they have no competing financial interests.

Correspondence and requests for materials should be addressed to M.H. (e-mail: holzenberger@st-antoine.inserm.fr).

Srb10/Cdk8 regulates yeast filamentous growth by phosphorylating the transcription factor Ste12

Chris Nelson, Susan Goto, Karen Lund, Wesley Hung & Ivan Sadowski

Department of Biochemistry and Molecular Biology, University of British Columbia, Vancouver, British Columbia V6T 1Z3, Canada

The budding yeast *Saccharomyces cerevisiae* differentiates into filamentous invasively growing forms under conditions of nutrient limitation^{1,2}. This response is dependent on the transcription factor Ste12 and on the mating pheromone-response mitogen-activated protein (MAP) kinase cascade¹, but a mechanism for regulation of Ste12 by nutrient limitation has not been defined. Here we show that Ste12 function in filamentous growth is regulated by the cyclin-dependent kinase Srb10 (also known as Cdk8), which is associated with the RNA polymerase II holoenzyme. Srb10 inhibits filamentous growth in cells growing in rich medium by phosphorylating Ste12 and decreasing its stability. Under conditions of limiting nitrogen, loss of Srb10 protein and kinase activity occurs, with a corresponding loss of Ste12 phosphorylation. Mutation of the Srb10-dependent phosphorylation sites increases pseudohyphal development but has no effect on the pheromone response of haploid yeast. Srb10 kinase activity is also regulated independently of the mating pheromone-response pathway. This indicates that Srb10 controls Ste12 activity for filamentous growth in response to nitrogen limitation and is consistent with the hypothesis that Srb10 regulates gene-specific activators in response to physiological signals to coordinate gene expression with growth potential.

Yeast differentiate into elongated invasively growing filamentous forms to facilitate foraging under conditions of nitrogen or carbon limitation^{1,2}. This response requires the transcription factors Ste12 and Tec1, which bind cooperatively to filamentous response elements (FREs) within the promoters of filamentous response genes³. Transcription from FREs is induced in response to nitrogen starvation⁴, and filamentous response requires upstream signalling components of the MAP kinase pheromone-response pathway, but a mechanism for regulation of Ste12 by nutrient limitation has not been identified.

Yeast lacking the RNA polymerase II holoenzyme-associated cyclin-dependent kinase (CDK) Srb10 show increased expression of Ste12-dependent filamentous responsive genes (ref. 5 and Fig. 1a), form more extensive pseudohyphae in nitrogen-depleted (SLAD) medium (Fig. 1b) and show constitutive pseudohyphae even on rich medium (data not shown). This effect is dependent on *STE12*, because diploid yeast with disruptions of both *srb10* and *ste12* do not form pseudohyphae on nitrogen-limiting medium (Fig. 1b, *srb10, ste12*) and have barely detectable levels of FRE-

dependent transcription (Fig. 1a). Disruption of *ste11*, which encodes the pheromone-responsive MAP/extracellular-signal-regulated kinase (ERK) kinase kinase (MEKK), also prevents filamentous growth (Fig. 1b) and FRE-dependent transcription (Fig. 1a) in *srb10* yeast. Therefore, elimination of Ste12 activity, by either gene disruption or impairing basal signalling, prevents the hyperfilamentous response of yeast lacking Srb10, suggesting that Srb10 may inhibit filamentous growth by modulating the activity of Ste12.

Consistent with this possibility, we found that Ste12 is a substrate for purified recombinant Srb10–Srb11 (Cdk8–cyclinC) complexes *in vitro* (Fig. 1c). Wild-type Srb10–Srb11 complexes phosphorylated recombinant Ste12 (Fig. 1c, lane 1), but not the inhibitors Dig1 and Dig2 (lanes 3 and 4). By contrast, a mutant Srb10 protein with impaired kinase activity (Asp290Ala)⁵ only weakly phosphorylated Ste12 *in vitro* and also underwent inefficient autophosphorylation (Fig. 1c, lane 2). Ste12 was phosphorylated on two peptides by Srb10 *in vitro* (Fig. 1d, peptides 3 and 4); these peptides co-migrated with phosphopeptides 3 and 4 derived from Ste12 labelled *in vivo* (ref. 6,

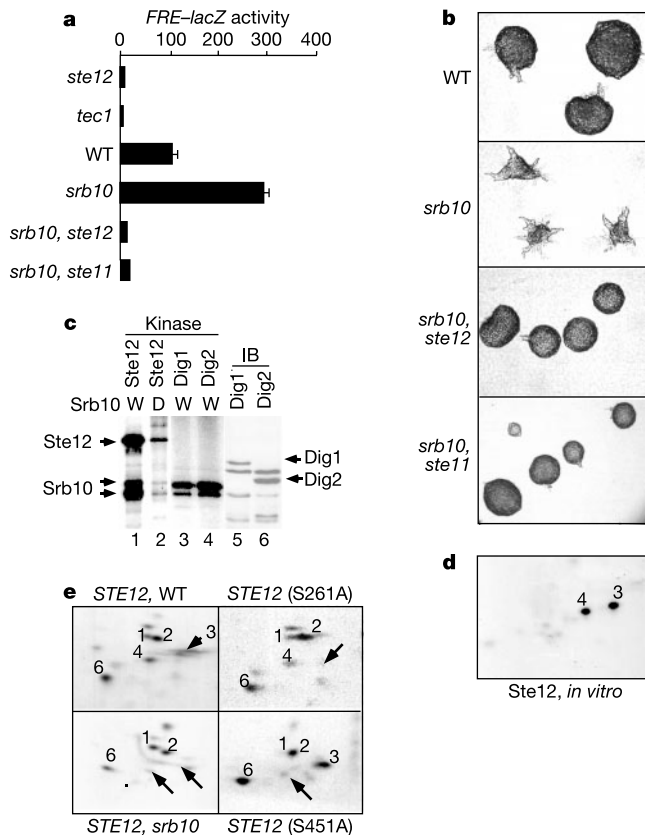


Figure 1 Phosphorylation of Ste12 by Srb10 inhibits filamentous responsive transcription. **a**, Deletion of *srb10* increases FRE-dependent transcription. Homozygous diploid strains bearing an *FRE-lacZ* reporter³ were grown at 30 °C in selective media and assayed for β -galactosidase activity⁹. **b**, Hyperfilamentation of *srb10* strains requires *STE12* and an intact MAPK cascade. Homozygous diploid yeast were streaked on SLAD plates and photographed after 3 d. **c**, Srb10 phosphorylates Ste12 *in vitro*. Kinase reactions were carried out with purified recombinant wild-type Srb10–Srb11 (ref. 12; lanes 1, 3, 4) or a kinase-deficient Asp290Ala Srb10–Srb11 mutant (lane 2) plus recombinant Ste12 (lanes 1, 2), GST–Dig1 (lane 3) or GST–Dig2 (lane 4). Input substrate GST–Dig1 and GST–Dig2 proteins were immunoblotted with antibodies to GST (lanes 5, 6). **d**, Srb10 phosphorylates two sites on Ste12. Tryptic phosphopeptide analysis of *in vitro* phosphorylated Ste12 was done as described⁶. The resulting peptides co-migrate with Ste12 phosphopeptides 3 and 4 (not shown). **e**, Srb10 is required for phosphorylation of Ser 261 and Ser 451 in Ste12 *in vivo*. Shown is tryptic phosphopeptide analysis of *in vivo* phosphorylated Ste12 recovered from wild-type or *srb10* strains expressing wild-type *STE12* (left panels), S261A *STE12* (top right) or S451A *STE12* (bottom right).